

DATA-BASED NONLINEAR AEROELASTIC MODELING

Dario H. Baldelli[†], Rick Lind[‡], Marty Brenner[§]

[†]ZONA Technology, Inc., [‡]University of Florida, [§]NASA Dryden Flight Research Center

Keywords: *Flight-Test Data, AE/ASE Models, Block-Oriented Models, LCO, Flutter.*

Abstract

The investigation of flutter and aeroservoelastic stability through flight testing is an essential part of aircraft certification. The stability boundary prediction is especially difficult when the instability is associated with nonlinearity in the dynamics. This paper presents an approach for the characterization of the nonlinear dynamics by non-iterative identification algorithms. Two different block-oriented nonlinear models are considered in this work to augment existing linear models with nonlinear operators derived by analyzing flight data. Central in the identification of block-oriented nonlinear models is the use of the a-priori set of orthonormal bases tuned with the dynamics of the aeroelastic/aeroservoelastic plant. In both cases, we propose a method to generate the orthonormal bases that is based on the cascade of input-normal balanced state-space realizations of all-pass filters. Case studies using a simulated structurally nonlinear prototypical two-dimensional wing section and actual F/A-18 AAW Ground Vibration Test (GVT) data are presented.

1 Introduction

Recently there has been intense research activity in nonlinear modeling and analysis for aeroelastic/aeroservoelastic (AE/ASE) systems within the flight test community, [3], [11]. Some of the current generation fighter aircraft carrying external stores are sensitive to develop a sort of nonlinear oscillation in the high subsonic to low supersonic speed regime, [4], [10]. Linear flutter engineering tools only are able to predict divergent oscillations while the observed in flight dynamic behavior is of limited amplitude. Hence,

some kind of nonlinear AE/ASE modeling capability must be developed in order to explain in-flight observed nonlinear dynamic behavior.

This work proposes the estimation of the observed nonlinear dynamics within an interconnected feedback framework, where the unknown dynamics turn out to be a function of the measured state vector, $x(t)$, and/or the measured input vector, $u(t)$, of the AE/ASE model. To this end a class of nonlinear models called *block-oriented*, which consists of the interconnection of Linear Time Invariant (LTI) systems and memoryless nonlinearities, are used. In particular, this paper focuses on the identification of Hammerstein and Wiener models from a N -point data record of observed input-output measurements from an AE/ASE system.

The approach adopted here is motivated by Gómez, *et al.*, [6], and the implemented identification algorithms are non-iterative. Specific identification strategies are formulated in accordance with the nature of the available data set. A Hammerstein model identification approach is applied when measurements at the input of the unknown nonlinear map are accessible, otherwise a Wiener method is suggested, (sensor nonlinearity). The identification algorithms are composed of Least Square Estimation (LSE) and Singular Value Decomposition (SVD) stages. The SVD technique is used to compute the solution of the associated 2-norm minimization problem.

The focus of this work seeks to augment existing linear models with nonlinear operators derived by analyzing flight-test data. Thus, these models would be suitable for analyzing aeroelasticity/aeroservoelasticity if the unknown non-

linearities could be included. Promising results were obtained when this data-based modeling approach was applied to a structurally nonlinear two-dimensional wing section as well as a set of F-18/AAW GVT data. The outcomes indicate that this setup reproduces, with a high degree of fidelity, the nonlinear dynamic behavior present in the observed measurement set.

2 Nonlinear Aeroelastic Feedback System

In reference [7] a general AE/ASE nonlinear feedback setup for identification purposes is established. In particular, the proposed interconnected nonlinear feedback framework allows an expedient and efficient estimation of the unknown dynamics, or errors from flight data measurements. In the devised setup, the unknown dynamics are denoted by the operator $X(z)$, being $z(t)$ a function of the measured state vector $x(t)$ and/or the measured input vector $u(t)$ of the AE/ASE model.

Specific formulations were derived for two different unmodeled dynamic identification scenarios. One scenario assumes that the unknown dynamics is purely a function of the measured states, $X(z) = X(x)$, while the other assumes that the unknown dynamics is purely a function of the measurement inputs, $X(z) = X(u)$. In this paper the former scenario is discussed whereas the latter was presented in [1]. Let's consider the generalized AE/ASE equation of motion,

$$M\ddot{x} + C\dot{x} + Kx - Fu = X(z) \quad (1)$$

where $x(t) \in \mathbb{R}^{n_x}$ and $u(t) \in \mathbb{R}^{n_u}$. The additional signal $z(t) \in \mathbb{R}^{n_z}$ is dimensioned such that $X: \mathbb{R}^{n_z} \rightarrow \mathbb{R}^{n_x}$, is in general a nonlinear mapping of appropriate dimension. As shown in Figure 1, this model is now represented as a nonlinear data-sampled feedback LFT,

$$y_k = F_l[P, X(z_k)]u_k \quad (2)$$

$$P = \begin{bmatrix} P_{11} & P_{12} \\ P_{21} & P_{22} \end{bmatrix} \quad (3)$$

where P is the nominal plant and P_{ij} , $i, j = 1, 2$ are the transfer functions related to the input

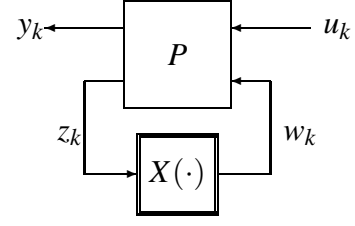


Fig. 1 Generic Nonlinear Feedback Framework.

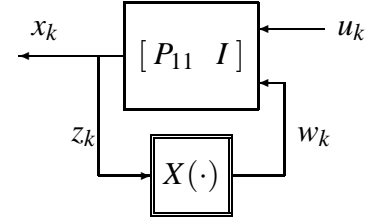


Fig. 2 LFT with Unmodeled Dynamic $X(x)$.

and output signals, respectively. These transfer function matrices are functions of the M , C , K and F matrices of the AE/ASE model described by equation (1). Finally, the known and unknown elements of the model are related through a feedback interconnection by the discrete-time signal $w_k = X(z_k)$. In this setup the identification procedure focuses on the case where the signal z_k is measured and can be inferred only from the knowledge of the measured output \bar{y}_k . This means that measurements at the input of the possible nonlinear dynamic $X(x_k)$ are accessible. Let's consider that the complete state vector, x_k , is available from the measured output, i.e., $x_k \equiv \bar{y}_k$, then

$$x_k = F_l(P, X(x_k))u_k \quad (4)$$

Consequently, we can express the relationship as,

$$x_k = P_{11}u_k + X(x_k) \quad (5)$$

where $P_{11}u_k$ characterizes the linear component of the measured output signal x_k , and in what follows it is assumed that $P_{12} = I$ as shown in Figure 2. The key point is to visualize that the unmodeled dynamic, $X(x_k)$, will give rise to a nonlinear operator which can be replaced with the Hammerstein model $X(x_k) = GN(x_k)$ or a Wiener Model $X(v_k)$, with the signal $v_k = Gx_k$, respectively. This model presents a clearly visible block

structure of a memoryless nonlinear gain and a LTI system in cascade connection.

2.1 Nonlinear Aeroelastic Feedback System Using Block-Oriented Models

The proposed interconnected nonlinear feedback model shown in Figure 1 results in an extension of LFT models and it can be used to model systems which exhibit hysteresis, limit cycles, sub-harmonics, jump resonances and nonlinear damping.

In this section we employed *block-oriented* models to augment existing linear models with nonlinear operators derived by analyzing flight data. They consist of the interconnection of a LTI system with a memoryless nonlinearity. Several combinations of these two elements are possible, hence giving rise to a set of different models. A model with a static nonlinearity at the input is called a Hammerstein model and it can be associated with nonlinear actuators in the AE/ASE system. A Wiener model is defined if the static nonlinearity is located at the output and this can be the case if the AE/ASE system has sensors with nonlinear behavior.

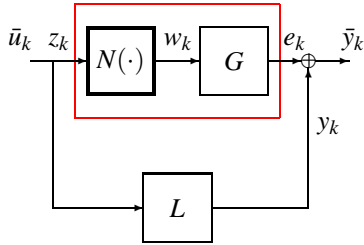


Fig. 3 Nonlinear LFT Modeling of \bar{y}_k using a Hammerstein Model.

Figures 3 and 4 show the nonlinear measured response, \bar{y}_k , as a result of adding the output, y_k , from the linearized discrete-time model, $L(z)$, with the error signal, e_k , coming from a Hammerstein, or Wiener nonlinear models, respectively. In addition, these figures show the input and output signals related with the nominal plant, P , and the nonlinearity, $X(\cdot)$, in the LFT representation depicted in Figure 2. Specifically, the standard

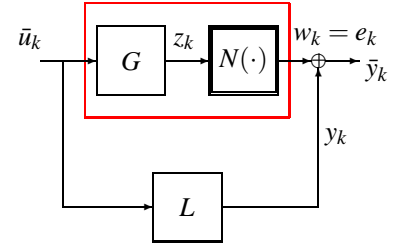


Fig. 4 Nonlinear LFT Modeling of \bar{y}_k using a Wiener Model.

plant P , associated with the two nonlinear models introduced earlier is,

- Hammerstein Model, P_H :

$$P_H = \begin{bmatrix} L & G \\ I & 0 \end{bmatrix} \quad (6)$$

- Wiener Model, P_W :

$$P_W = \begin{bmatrix} L & I \\ G & 0 \end{bmatrix} \quad (7)$$

where the linear and nonlinear blocks are,

$$G(q) = \sum_{l=0}^{p-1} b_l B_l(q) \quad (8)$$

$$N(\cdot) = \sum_{i=1}^r \alpha_i g_i(\cdot) \quad (9)$$

In the last set of equations, $\alpha_i \in \mathbb{R}^{n \times n}$, ($i = 1, \dots, r$), and $b_l \in \mathbb{R}^{m \times n}$, ($l = 0, \dots, p-1$) are the unknown parameters for both blocks. The signals z_k and w_k are incorporated in order to relate the nonlinearity to the nominal linear plant in a feedback interconnection. By closing the lower loop in Figure 2, the input-output behavior using the previous nonlinear models –shown in Figures 3 and 4– are,

- LFT using a Hammerstein Model P_H :

$$\bar{y}_k = F_l [P_H, N(z_k)] = (L + GN(z_k)) \bar{u}_k \quad (10)$$

- LFT using a Wiener Model P_W :

$$\bar{y}_k = F_l [P_W, N(z_k)] = (L + N(z_k)G) \bar{u}_k \quad (11)$$

Central in the identification of block-oriented nonlinear models is the use of the *a-priori* set of orthonormal bases, $\{B_l(q)\}_{l=0}^{p-1}$, in equation (8) tuned with main dynamics of the plant. This could be extracted from the *a-priori* linear model $P_{11} = L$ or from the *a-posteriori* experimental evidence, such as wind-tunnel, GVT or flight-test data of the AE/ASE system.

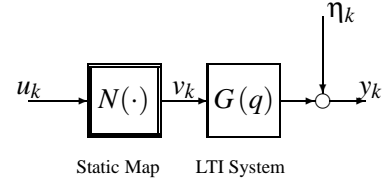


Fig. 5 MIMO Hammerstein Model.

3 Block-Oriented Nonlinear Identification

Nonlinearities in actuators and sensors can be represented by the interconnection of static nonlinearities and LTI systems. For such plants, a nonlinear system identification approach using a set of tuned orthonormal basis functions is proposed in this section.

3.1 Hammerstein Model Identification

Consider the multivariable Hammerstein nonlinear model shown in Figure 5. The model consist of a static nonlinearity, $N(\cdot)$,

$$N(\cdot) = \sum_{i=1}^r \alpha_i g_i(\cdot) \quad (12)$$

in series connection with a LTI system described by its transfer function matrix,

$$G(q) = \sum_{l=0}^{p-1} b_l B_l(q) \quad (13)$$

where $G(q) \in \mathbf{H}_2^{m \times n}(\mathbb{T})$, and \mathbb{T} denotes the unit circle, $\mathbb{T} = \{z \in \mathbb{C} : \|z\| = 1\}$. In this case, $y_k \in \mathbb{R}^m$, $u_k \in \mathbb{R}^n$, and $\eta_k \in \mathbb{R}^m$ represent the system output, input and measurement noise vectors at time k , respectively. The input-output relationship, shown in Figure 5, is then given by

$$y_k = G(q)N(u_k) + \eta_k \quad (14)$$

Substituting Eqs (13) and (12) in (14), the input-output relationship is written as,

$$y_k = \sum_{l=0}^{p-1} \sum_{i=1}^r b_l \alpha_i B_l(q) g_i(y_k) + \eta_k \quad (15)$$

As noted in reference [6] a unique parameterization is obtained if the parameter matrices α_i is normalized, that is $\|\alpha_i\|_2 = 1$. Lets now define,

$$\theta \triangleq [b_0 \alpha_1, \dots, b_0 \alpha_r, \dots, b_{p-1} \alpha_1, \dots, b_{p-1} \alpha_r]^T \quad (16)$$

$$\phi_k \triangleq [B_0(q)g_1^T(y_k), \dots, B_0(q)g_r^T(y_k), \dots, B_{p-1}(q)g_1^T(y_k), \dots, B_{p-1}(q)g_r^T(y_k)]^T \quad (17)$$

substituting Eqs (16) and (17) in (15), the latter results in the regression form,

$$y_k = \theta^T \phi_k + \eta_k \quad (18)$$

Now, with the data set $\{u_k, y_k\}_{k=1}^N$ and defining $Y_N \triangleq [y_1^T, \dots, y_N^T]$, $\Gamma_N \triangleq [\eta_1^T, \dots, \eta_N^T]$ and $\Phi_N \triangleq [\phi_1, \dots, \phi_N]$, we obtain,

$$Y_N = \Phi_N^T \theta + \Gamma_N \quad (19)$$

Using the least squares criterion, an estimate $\hat{\theta}$ of θ is obtained as

$$\hat{\theta} = (\Phi_N \Phi_N^T)^{-1} \Phi_N Y_N = \Phi_N^\dagger Y_N \quad (20)$$

if the inverse exists. Defining Θ_{ab} as

$$\Theta_{ab} \begin{bmatrix} \alpha_1^T b_0^T & \dots & \alpha_1^T b_{p-1}^T \\ \vdots & \dots & \vdots \\ \alpha_r^T b_0^T & \dots & \alpha_r^T b_{p-1}^T \end{bmatrix} = \alpha b^T \quad (21)$$

with $\alpha \triangleq [\alpha_1, \dots, \alpha_r]^T$, and $b \triangleq [b_0^T, \dots, b_{p-1}^T]$, the parameter matrix can be expressed as, $\theta = \text{blockvec}(\Theta_{ab})$. Then, an estimate of $\hat{\alpha}$ and \hat{b} can be obtained from the estimate of $\hat{\Theta}_{ab}$. The solution is given by solving the 2-norm minimization problem,

$$(\hat{\alpha}, \hat{b}) = \arg \min_{\alpha, b} \{\|\Theta_{ab} - \alpha b^T\|_2^2\} \quad (22)$$

The following result provides the solution to this optimization problem through the SVD of $\hat{\Theta}_{ab}$, [5]. Let $\hat{\Theta}_{ab} \in \mathbb{R}^{nr \times mp}$ have rank $k > n$, and let its economy size SVD be partitioned as

$$\begin{aligned}\hat{\Theta}_{ab} &= U_k \Sigma_k V_k^T = \sum_{i=1}^s \sigma_i u_i v_i^T \\ &= [U_1 \ U_2] \begin{bmatrix} \Sigma_1 & 0 \\ 0 & \Sigma_2 \end{bmatrix} \begin{bmatrix} V_1^T \\ V_2^T \end{bmatrix}\end{aligned}\quad (23)$$

with $U_1 \in \mathbb{R}^{nr \times n}$, $V_1 \in \mathbb{R}^{mp \times n}$, and $\Sigma_1 = \text{diag}(\sigma_1, \sigma_2, \dots, \sigma_n)$. Then,

$$(\hat{\alpha}, \hat{b}) = \arg \min_{\alpha, b} \|\hat{\Theta}_{ab} - \alpha^T b\|_2^2 = (U_1, V_1 \Sigma_1) \quad (24)$$

3.2 Wiener Model Identification

A block scheme of a process with output nonlinearity in *input-output* representation is shown in Figure 6, and it can be considered as a special case of the Volterra series. In this figure $y_k \in \mathbb{R}^m$, $u_k \in \mathbb{R}^n$, and $\eta_k \in \mathbb{R}^m$ represent the system output, input and process noise vectors at time k , respectively. Lets now consider the multi-variable

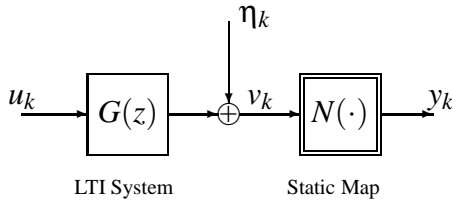


Fig. 6 Wiener Model Structure.

feedback nonlinear model which consist of a LTI system described by equation (13). The nonlinear function $N(\cdot) : \mathbb{R}^m \rightarrow \mathbb{R}^m$ is assumed to be invertible and given by

$$N^{-1}(y_k) = \sum_{i=1}^r \alpha_i g_i(y_k) \quad (25)$$

where $g_i(\cdot) : \mathbb{R}^m \rightarrow \mathbb{R}^m$, ($i = 1, \dots, r$), is the assumed basis functions which typically turn out to be a polynomial and $\alpha_i \in \mathbb{R}^{m \times m}$, ($i = 1, \dots, r$), is the unknown matrix parameters. In what follows it will be assumed that $a_1 = I_m$.

The Wiener model identification problem is then to estimate the unknown parameter matrices α_i , ($i = 1, \dots, r$), and b_l , ($l = 0, \dots, p-1$) characterizing the nonlinear and linear parts from the N -point data record $\{u_k, y_k\}_{k=1}^N$ of observed input-output measurements, [6].

In Figure 6 the intermediate variable v_k can be written as,

$$v_k = G(q)u_k + \eta_k \quad (26)$$

in addition it can be expressed as,

$$v_k = N^{-1}(y_k) \quad (27)$$

By equating the RHS of both equations, and considering the parameterizations given by (13) and (12),

$$g_1(y_k) = - \sum_{i=2}^r \alpha_i g_i(y_k) + \sum_{l=0}^{p-1} b_l B_l(q) u_k + \eta_k \quad (28)$$

Now, lets define

$$\theta \triangleq [\alpha_2, \alpha_3, \dots, \alpha_r, b_0, b_1, \dots, b_{p-1}]^T \quad (29)$$

$$\begin{aligned}\phi_k \triangleq & [-g_2^T(y_k), -g_3^T(y_k) \dots, -g_r^T(y_k), \\ & B_0(q)u_k^T, \dots, B_{p-1}(q)u_k^T]^T\end{aligned}\quad (30)$$

and consequently (28) can be written in a linear regression form as,

$$g_1(y_k) = \theta^T \phi_k + \eta_k \quad (31)$$

By considering the data set $\{u_k, y_k\}_{k=1}^N$, and defining

$$\begin{aligned}Y_N &= [g_1(y_1)^T, \dots, g_1(y_N)^T]^T \\ \Gamma_N &= [\eta_1^T, \dots, \eta_N^T]^T \\ \Phi_N &= [\phi_1^T, \dots, \phi_N^T]^T\end{aligned}$$

we obtain

$$Y_N = \Phi_N^T \theta + \Gamma_N \quad (32)$$

Using the least squares criterion, it is well known that an estimate $\hat{\theta}$ of θ is obtained as

$$\hat{\theta} = (\Phi_N \Phi_N^T)^{-1} \Phi_N Y_N = \Phi_N^\dagger Y_N \quad (33)$$

Finally, the estimates parameters $\hat{\alpha}_i$, ($i = 2, \dots, r$), and \hat{b}_l , ($l = 0, \dots, p - 1$), results from the proper partition of $\hat{\theta}$ in equation (33), in accordance to its own definition in (29).

Finally, it must be noted that in equation (13) we assume that the transfer function matrix can be represented parametrically by a set of orthonormal basis functions $\{B_k(q)\}_{k=0}^{p-1}$ and this set of functions are now obtained from a cascade connection of two-parameters *Kautz* filters.

3.3 Orthonormal Function Set Generation and Modal Parameter Estimation

In this section we propose a technique to tune the LTI part in the Block-Oriented model setup with the dynamic coming from elastic modes of the linearized model P_{11} , using a high-fidelity software package such as ZAERO [13], or from some identified linear dynamics using the N -point data $\{u_k, y_k\}_{k=1}^N$.

A two-parameter *Kautz* model is proposed to generate the set of basis functions, [2]. Its minimal realization is defined as $H_j(z) = C_j(zI - A_j)^{-1}B_j + D_j$, with the eigenvalues of A_j lying inside the unit circle. A filter is *all-pass* if $H_i(z)H_i(z^{-1}) = 1$ and it is said to be orthonormal if its state-space realization (A_i, B_i, C_i, D_i) is input normal. Let $H_{Kautz}(b, c)$ be

$$H_{Kautz}(b, c) = \frac{-cz^2 + b(c-1)z + 1}{z^2 + b(c-1)z - c} \quad (34)$$

with $|b| < 1$ and $|c| < 1$, respectively. In reference [9] it was formalized that the series connection of orthonormal *all-pass* filters transfer both properties to the resulting filter. Then, it is possible to build a set of orthonormal basis functions from a family of stable *all-pass* filters with input normal realizations, that is

$$H(z) = \prod_{j=1}^s H_j(z) \quad (35)$$

whose state space input normal realization results

$$H(z) = C_n(zI - A)^{-1}B_n + D_n \quad (36)$$

with $p = \sum_{j=1}^s n_j$.

Now, let $x(t) = (x_0^T(t), \dots, x_s^T(t))^T$, be the state of the filter $H(z)$, where each component, x_j adopts the form $x_j(t) = (x_{1j}, \dots, x_{n_jj})^T$, for $j = 1, \dots, s$. Then the set of orthonormal basis are defined by the transfer functions, $B_k(q)$, from the filter input $u(t)$, to each of the filter state components $x_k(t)$ $k = 0, \dots, p - 1$,

$$\begin{aligned} x_k(t) &= B_k(q)u(t) \\ B_k(q) &= c_k(zI - A_n)^{-1}B_n \end{aligned} \quad (37)$$

with q being the forward shift: $qu(t) = u(t + 1)$ and c_k is the k -th Euclidean basis vector in \mathbb{R}^n .

Additionally, the set of *a-priori* basis functions used to describe the linear part $G(q)$ in Eq. (13) are tuned with the linear modal parameters contained in the the N -data record of experimental evidence $\{u_k, y_k\}_{k=1}^N$. Hence, a multistage eXogenous AutoRegressive Moving Average – ARMAX – procedure is applied, [8]. This technique is based on the coefficients of the ARMAX model that satisfy the maximum of the likelihood function corresponding to the experimental evidence. The first stage of the numerical algorithm involves the estimation of a long eXogenous AutoRegressive model, ARX. In the second stage, the coefficients of the ARMAX model are computed iteratively from their ARX ones.

4 Case Study 1: Nonlinear Pitch-Plunge Aeroelastic System

The selected case is a structurally nonlinear prototypical two-dimensional wing section. The nonlinearity included in the model is a memory-less quadratic gain affecting the stiffness of the pitch motion through the pitch rotation of the airfoil, ($k_{\alpha^2}\alpha^2$). The system parameters to be used in this numerical simulations as well as the general geometry of the aeroelastic model are given in reference [7].

The aeroelastic system matrices M , K , C and F are identical to those presented in reference [7]. In all considered cases the simulated measured system output is the pitch angle, α_k , – which is corrupted with a zero-mean Gaussian distributed white noise with standard deviation $\sigma = 0.01$ – and the system input is the flap deflection, β_k .

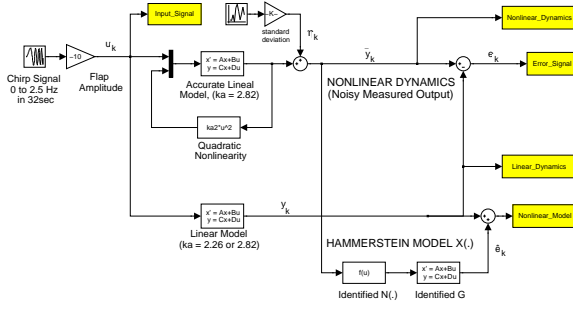
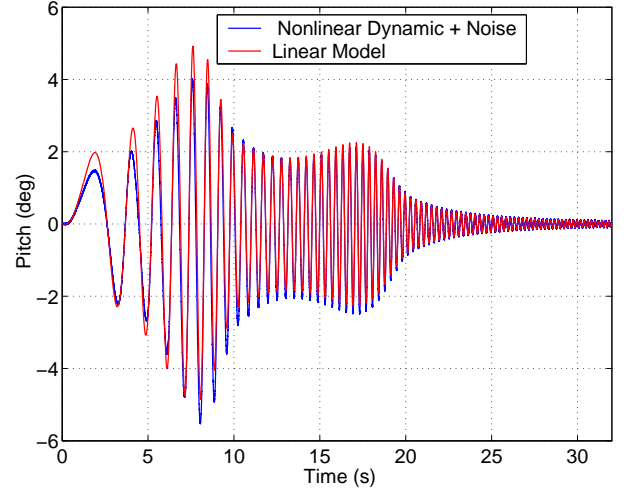


Fig. 7 Flowchart for the $X(\cdot)$ Estimation.

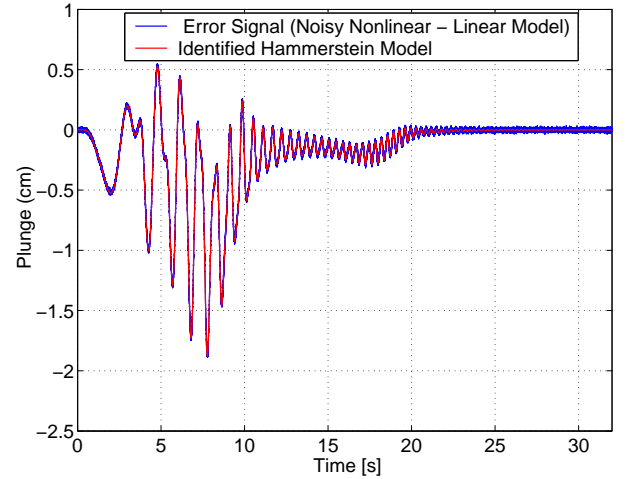
In what follows a noisy error signal, e_k , is defined as the difference between the measured signal, \bar{y}_k , (nonlinear dynamics), and the simulated linear part of the model, $y_k = P_{11}u_k$. The proposed nonlinear identification algorithm was employed to identify the unmodeled dynamics, from a N -point data of the noisy error signal, e_k , using a sampling frequency of 1000 Hz . In connection with the linear portion of the model, P_{11} , an explicit modeling error is incorporated by an inaccurate value of the pitch stiffness, k_α . Hence, an accurate linear model results when the nominal pitch stiffness equal to $k_\alpha = 2.82$ is used, while the inaccurate linear model is defined by $k_\alpha = 2.26$.

Figure 7 shows the flowchart model used to generate the simulated pitch deflection signal, $\bar{y}_k \equiv \alpha_k$, (nonlinear dynamics) as well as the response from the nonlinear model. It is clearly visible that the signal used to drive the Hammerstein model $X(\cdot)$ is the measured pitch, α_k , and that the output of this system is the error estimation \hat{e}_k of e_k . The linear model used in this case is an inaccurate one, (i.e. $k_\alpha = 2.26$) and its output is denoted by y_k . The nonlinear model response is finally obtained when the estimation error \hat{e}_k is added to y_k . Additionally, all simulation data needed in the nonlinear identification algorithm is saved through the denoted variables within the yellow boxes. Figure 8(a) shows in blue the nonlinear dynamic signal, \bar{y}_k , altogether with the response of the inaccurate linear model, y_k , in red.

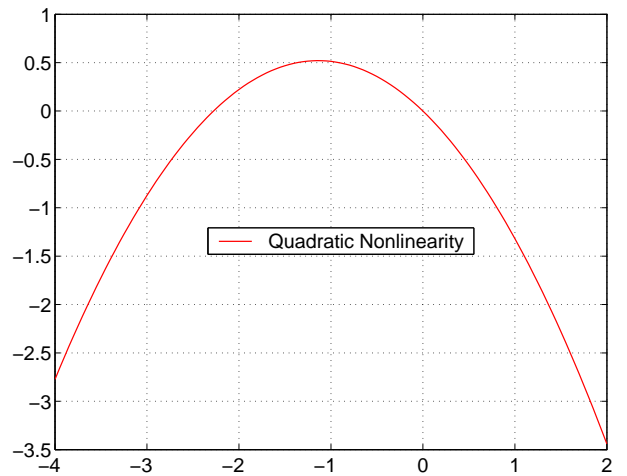
The difference between both signals, $e_k = \bar{y}_k - y_k$, is plotted in blue in Figure 8(b). From the dynamic of P_{11} , two *all-pass* Kautz filters are



(a) Response of Noisy Nonlinear Dynamics \bar{y}_k and Inaccurate Linear System y_k .



(b) Difference in Measurements from Noisy Nonlinear Dynamics and Inaccurate Linear model, blue: $e_k = \bar{y}_k - y_k$, red: \hat{e}_k .



(c) Identified Quadratic Nonlinearity, $N(u_k) = -0.9155u_k - 0.4022u_k^2$.

Fig. 8 Pitch-Plunge Aeroelastic System

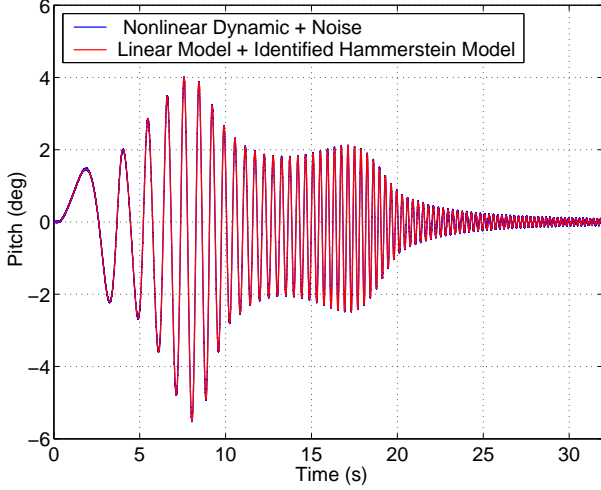


Fig. 9 Response of Noisy Nonlinear Dynamics \bar{y}_k and Nonlinear Model $y_k + \hat{e}_k$.

used to generate the required four basis function set $\{B_k(q)\}_{k=0}^3$. These are,

$$B_k(q) = \left[\begin{array}{cccc|c} 0.9998 & 0.0166 & 0 & 0 & 0 \\ -0.0166 & 0.9964 & 0 & 0 & 0.0831 \\ 0 & 0 & 0.9999 & 0.0067 & 0 \\ 0.0001 & 0.0065 & -0.0067 & 0.9969 & 0.0781 \\ \hline & c_k & & & 0 \end{array} \right] \quad (38)$$

where $c_k = [0 \ 1 \ 0 \ 0]$ with 1 in position k (k -th Euclidean basis vector in \mathbb{R}^4). The nonlinear identification algorithm is now used to compute the parameter vectors $\hat{\alpha}$ and \hat{b} defined in equation (21). The estimated \hat{b}_k coefficients for this case are: $\hat{b}_0 = 3.048 \times 10^{-3}$, $\hat{b}_1 = -2.6553 \times 10^{-3}$, $\hat{b}_2 = 1.7607 \times 10^{-3}$ and $\hat{b}_3 = 2.9988 \times 10^{-3}$, respectively.

Figure 8(b) shows in red the time trace of the output signal coming from the identified Hammerstein model $\hat{X}(\cdot)$. A good agreement between e_k and \hat{e}_k is obtained and it is almost impossible to distinguish one from the other. The identified quadratic map $\hat{N}(\cdot)$ is depicted in Figure 8(c) and its identified coefficients are $\hat{\alpha}_1 = -0.9155$ and $\hat{\alpha}_2 = -0.4022$. The inaccuracy of the known linear model, P_{11} , results in a noticeable displacement of the nonlinear map's origin from zero towards the left hand plane. This can be easily explained in terms of the magnitude of the estimate

coefficient $\hat{\alpha}_1$. The large magnitude of it clearly indicates that the assumed linear model, P_{11} , is a poor representation of the true linear dynamics. In other words, the estimated memoryless gain is trying to cover the undermodeling linear dynamics with a strong linear term coefficient, $\hat{\alpha}_1$.

Finally, Figure 9 presents in blue the time trace of the noisy simulated pitch response, \bar{y}_k , and in red the output from the identified Hammerstein model, y_k . Note that, besides the inaccurate linear model used to generate the basis function set $\{B_k(q)\}_{k=0}^3$, the nonlinear identification approach is able to reproduce with good fidelity the nonlinear behavior embedded in the output data, \bar{y}_k .

5 Case Study 2: F/A-18 AAW GVT Data Analysis

Ground vibration tests (GVT) were performed on the F/A-18 AAW aircraft to assess the structural characteristics of the modified airframe during the Phase I Flight Research, [12]. This subsection deals with the case of the F/A-18 AAW-ASE LTI model update by incorporating the unmodeled dynamics using a Wiener model computed from the acceleration error signal. This signal is defined as the difference between the measured GVT data $-n_{z100}$ and the predicted response coming from the ASE LTI model, N_z . As shown in Figure 2, this update process is represented as a nonlinear feedback Linear Fractional Transformation LFT between the ASE model denoted by P and the unmodeled dynamic, $X(\cdot)$. The latter is replaced by the estimated Wiener model. Figure 10 shows in blue the measured acceleration response, n_{z100} , altogether with the ASE model response, N_z , in red. The unmodeled dynamic used to estimate the Wiener model is computed from these time traces.

Six natural frequencies and damping ratios computed from the vertical GVT data using an ARMAX(22,21,22) model in the multistage process – with an initial ARX model of order 60 – are presented in Table 1. These modal parameters are used to tune the poles of the *a-priori* set of orthonormal basis functions, $\{B_l(q)\}_{l=0}^5$, built

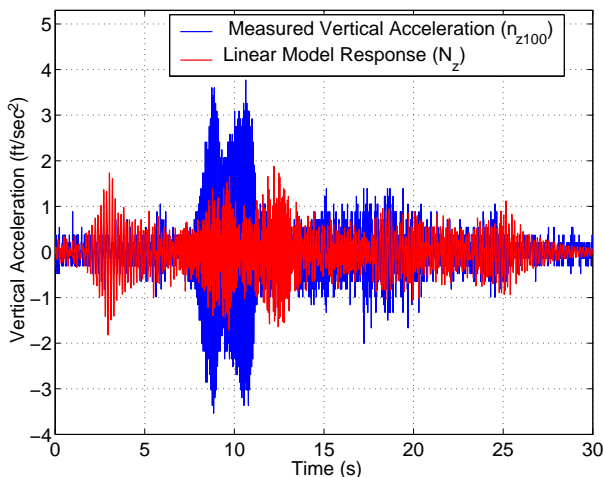


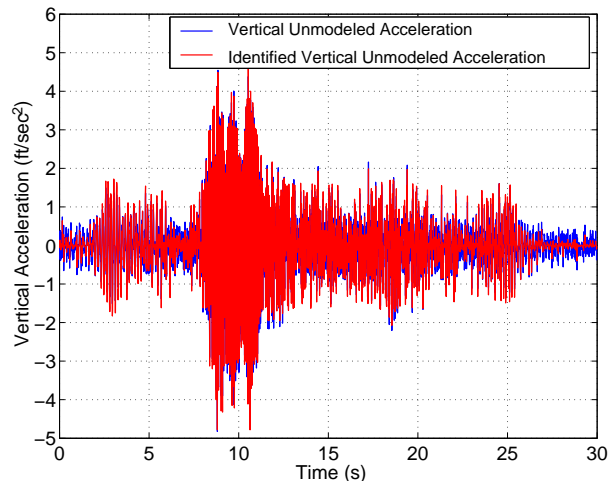
Fig. 10 F-18 AAW / GVT Measured and Analytical Linear Vertical Acceleration

through a series connection of two-parameter *Kautz* filters.

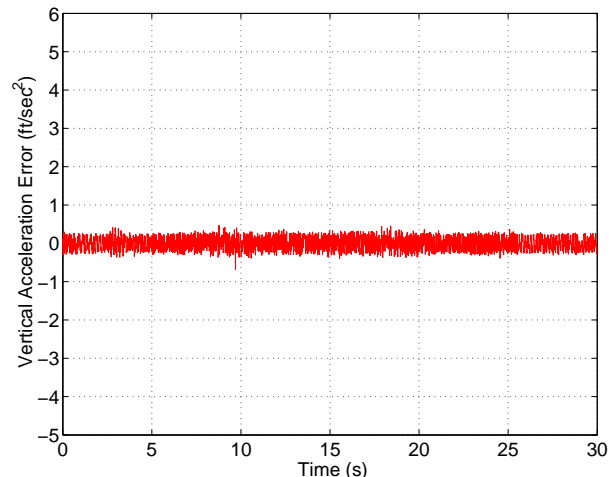
Table 1 F/A-18 AAW – Modal Parameters Identified from Unmodeled Vertical Dynamics

Mode	Natural Frequency f_i – [Hz]	Damping Ratio ζ_i
# 1	6.3079	1.4143×10^{-2}
# 2	9.6777	3.6278×10^{-2}
# 3	13.7698	3.2878×10^{-2}
# 4	15.8485	4.0317×10^{-2}
# 5	18.3387	1.3807×10^{-2}
# 6	20.6243	2.1379×10^{-2}

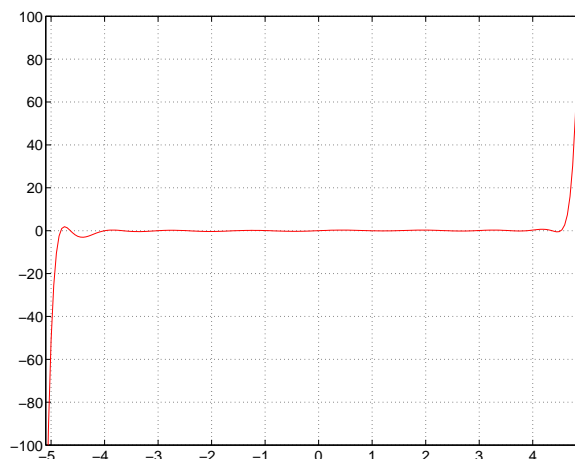
The predicted response from the Wiener model is shown in red in Figure 11(a) and is shown to compare quite closely with the unmodeled vertical signal (blue). The identified Wiener model is built with a LTI block of order 12, followed by a polynomial nonlinearity of order 17. The identification error is depicted in Figure 11(b). Its behavior is assumed to be linked with the measurement noise present in the GVT data. Figure 11(c) shows the identified memoryless nonlinearity from the 17th order polynomial.



(a) GVT Measured and Identified Vertical Unmodeled Acceleration



(b) Vertical Acceleration Error Signal



(c) Identified Vertical Dynamic Static-Map (Freeplay)

Fig. 11 F-18 AAW / GVT Measured and Identified Vertical Unmodeled Acceleration

6 Conclusions

In this paper we consider the identification of block-oriented models of AE/ASE dynamics. In particular, the approach sought to augment existing linear models with nonlinear operators derived by analyzing test data. Such an approach is warranted because commercial packages, such as ZAERO, are currently able to generate linear models with high levels of accuracy. Thus, these models would be suitable for analyzing aeroelasticity/aeroservoelasticity if the unknown nonlinearities could be included. Knowledge of the physics behind these nonlinearities is not yet mature so using flight data to identify the nonlinearities is the best approach. Furthermore, if the identified nonlinearity can be replaced by its Single Input Describing Function (SIDF), the resulting models can be used to compute robust stability margins using the μ -method that would reflect both flutter and LCO instabilities regions of the flight envelope.

7 Acknowledgement

Research supported by NASA Dryden Flight Research Center under STTR Phase I, NAS4-03014.

References

- [1] Baldelli, D.H., Chen, P.C., Liu, D.D., Lind, R., and Brenner, M., "Nonlinear Aeroelastic Modeling by Block-Oriented Identification," *45th AIAA/ASME/ASCE/AHS/ASC Structures, Structural Dynamics & Materials Conference*, AIAA Paper 2004-1938, April 19–22, 2004, Palm Springs, CA.
- [2] Bodin, P., Oliveira e Silva, T., and Wahlberg, B., "On the Construction of Orthonormal Basis Functions for System Identification," *13th Triennial World Congress, IFAC 1996*, pp. 369-374, 3a-12-3, San Francisco, CA, USA.
- [3] Brenner, M., and Prazenica, R.J., "Aeroservoelastic Model Validation and Test Data Analysis of the F/A-18 Active Aeroelastic Wing," *International Forum on Aeroelasticity and Structural Dynamics*, IFASD-US-32, June 2003.
- [4] Bunton, R.W., and Denegri Jr., C.M., "Limit Cycle Oscillation Characteristics of Fighter Aircraft," *Journal of Aircraft*, Vol. 37, No. 5, September-October 2000, pp. 916-918.
- [5] Golub, G.H., and Van Loan, C.F., "Matrix Computations," The Johns Hopkins University Press, Third Edition, 1996.
- [6] Gómez, J.C., and Baeyens, E., "Identification of Nonlinear Systems Using Orthonormal Bases," *Proceedings of the IASTED International Conference on Intelligent Systems and Control*, ISC 2001, Tampa, Florida, U.S.A., pp. 126-131, November 2001.
- [7] Lind, R., Prazenica R.J., and Brenner, M.J., "Estimating Nonlinearity Using Volterra Kernels in Feedback with Linear Models," *44th AIAA/ASME/ASCE/AHS Structures, Structural Dynamics, and Materials Conference*, 7-10 April 2003, Norfolk, Virginia, Paper AIAA-2003-1406.
- [8] Mignolet, M.P., and Red-Horse, J.R., "ARMAX Identification of Vibrating Structures: Model and Model Order Estimation," AIAA-94-1525-CP, *Proceedings of the 35th AIAA/ASME/ASCE/AHS/ASC Structures, Structural Dynamics, and Materials Conference* April 18-20, 1994, Hilton Head, SC, pp. 1628–1637.
- [9] Mullis, C.T., and Roberts, R.A., "Digital Signal Processing," *Addison-Wesley Series in Electrical Engineering*, Reading, MA, Addison-Wesley, 1987.
- [10] Norton, W.J., "Limit Cycle Oscillation and Flight Flutter Testing," *Proceedings of the Society of Flight Test Engineers 21st Annual Symposium*, 1990.
- [11] Prazenica, R.J., Brenner, M.J., and Lind, R., "Nonlinear Volterra Kernel Identification for the F/A-18 Active Aeroelastic Wing," *International Forum on Aeroelasticity and Structural Dynamics*, IFASD-US-32, June 2003.
- [12] Voracek, D., Pendleton, E., Reichenbach, E., Griffin, K., and Welch, L., "The Active Aeroelastic Wing Phase I Flight Research Through January 2003," *NASA/TM-2003-210741*.
- [13] ZAERO User's Manual, Version 7.0, ZONA Technology Inc., Scottsdale, AZ, www@zonatech.com, November 2003.